On Electrical Impedance Scanning – Principles and Simulations

B. Scholz[1], R. Anderson[2]

[1] *Siemens AG, Medical Engineering Group, Erlangen, Germany*
[2] *Siemens-Elema AB, Solna, Sweden*

Introduction

Various medical technologies are used to diagnose malignancy. For breast imaging, Mammography is the most widely accepted technique (in some countries, implemented in the form of screening of the healthy female population in accordance with established inclusion criteria). Mammography is practical as measured by its achievable performance, fast patient throughput and established standards. Ultrasound is the most common adjunct, especially useful for the examination of young women with dense breast tissue and in distinguishing cystic versus solid lesion composition. Magnetic Resonance Imaging, yielding a very high sensitivity but at the cost of a lower specificity, is more time-consuming and expensive, although a procedure of choice for certain indications, such as for women with implants or suspected multifocal carcinoma.

Other techniques, including thermal imaging and optical mammography, have been and continue to be researched. The technique considered in this manuscript, new as a modality but based on long-known principles, is Electrical Impedance Scanning (EIS). Currently being evaluated in multiple clinical studies worldwide, EIS may, on account of its potential to measure electrical properties and thereby offer information for tissue characterization, prove to be a useful adjunct to the breast care protocol.

EIS is based upon tissue-specific transmission of electrical low-level currents due to tissue-specific conductivities and permittivities. Recent *in vitro* measurements of electrical properties of breast tissue show that malignant tissue has higher electrical conductivity than healthy tissue [1-4]. The very rare *in vivo* impedance measurements support the findings [5, 6]. Changed electrical proper-ties of malignant tissue with respect to healthy tissue are attributed to increased cellular water and salt content, altered membrane permeability, changed packing density and orientation of cells [7-9].

Measurement Principle

Electrical impedance scanning measurements are based upon the tissue-specific electric field distribution and upon the measureability of related quantities – either currents or potentials – on the surface of the body at the region of interest. Due to the fact that the electrical impedance breast scanner TransScan TS2000 measures only currents, throughout this article, we restrict our discussion to the measurement of currents.

A cancerous lesion is assumed to have higher conductivity[1] than surrounding tissue. Therefore, in an equivalent circuit model for breast tissue, a cancerous lesion can be related to a resistor with a lower resistance or a higher conductance[2], respectively, than its surrounding. It attracts electrical field lines and thus enhances the current density through the lesion. After leaving the lesion, the current density gradually becomes uniform over distance, provided the medium has a uniform conductivity. Other sources which could also generate non-uniform current density distributions, will not be addressed in this and the following considerations.

Measuring currents with an array of closely spaced electrodes sufficiently near to the lesion allows detection of non-uniform current distribution, i. e. the distortion of the electric field due to the lesion. With such measurements, also multiple lesions can be detected, as long as the lesion-induced non-uniform distributions of currents hold present at the measurement sites. A lesion with lower conductivity than the surrounding tissue shows up as a hollow in the current map. Thus, the detectability of a focal region is a function of the depth, the size and the conductivity ratio of the focal region and its surrounding.

With increasing depth the lesion signal appears with less contrast since – as mentioned – the lesion-induced field distortions gradually fade to disappearance over distance.

[1] Conductivity σ is a specific quantity. Its SI dimension is $1/\Omega m = S/m$, $S = Siemens$. The resistance R of a sample is given by $R = l/(\sigma A)$, where l is the length and A is the cross-sectional area of this sample.

[2] Conductance is defined as the inverse of resistance. Its dimension is $S = 1/\Omega$.

A lesion large in lateral dimensions – constant size in depth direction assumed – causes current density which is uniform in its central part, and non-uniform at the lateral boundaries. At sufficient lateral distance to the lesion the current density is again uniform, but at a lower level. A large lesion is theoretically detectable if this inhomogeneous distribution of currents can be measured. This measurement depends on the size of the measurement area. From the perspective of the physical principles, large lesions – even if not deep – would not be expected to be electrically "visible" if the current line distortions from the lateral boundaries are not covered by the sensing probe. On the other hand, large lesions can be "visible" even when not covered by the probe. This may happen when the current distortions from the boundaries have "propagated" sufficiently sidewards. Such cases have occurred in clinical studies.

The dependence of lesion detectability on the conductivity ratio between lesion and adjacent tissue is basic to EIS. A decreasing ratio results in less distorted field lines, thus reducing the measurability of the lesion. As will be discussed in the next section, conductivities of living tissue are not reliably known. Actually, only *in vitro* data are available in the literature.

In addition to the magnitude of the alternating current, electrode-position dependent phase shifts of the currents can also be measured and mapped on a two-dimensional array. These phase shifts are related to the permittivity, i. e. the dielectric properties of different tissue regions transversed by the currents.

The measurement of two independent quantities enables presentation of two independent two-dimensional signal distributions, loosely described as two different "images". However, the aim of EIS is to obtain detection signals, i. e. localized enhancements of the volume current density from a lesion if there would be one. It is not the aim to produce an anatomical "image". The display of these signals, as electrical impedance "maps", will be discussed in connection with the numerical simulations and the TransScan TS2000 system.

Biophysics

In biological tissue, the electric field distribution, as well as the associated electrical current, depend on the electrical properties of the tissues under consideration. They can be described by electrical conductivity σ_s and dielectric permittivity ε. The permittivity depends on the frequency of the electric field whereas the conductivity σ_s is static. Both parameters are related to different physical mechanisms to be discussed.

The conductivity is a measure of the mobility of ions in the extracellular fluid in the presence of an electric field. The tissue composition (ratio of extracellular to intracellular volume) determines travel of current; therefore, electrical conductivity is tissue-specific.

Permittivity is related to polarization of media. Time-varying polarizations due to time-dependent electric fields cause polarization currents. The polarization processes involved are displacement and orientation polarization. In the frequency range of bioimpedance measurements (up to the MHz range), displacements of electron clouds with respect to their nuclei and of positive ions with respect to negative ions in large molecules are instantaneous. The orientation polarization of existing dipoles of different sizes, formed by cells or molecules, are time-delayed due to relaxation processes. They introduce phase shifts with respect to the applied time-varying electric field. For the ease of simpler calculations, polarization processes including relaxation are commonly described by a complex permittivity, relating the polarization and electric field vectors, also considered to be complex[3].

Assuming a time-dependent electric field oscillating with frequency ω, the electric current $\vec{j}$ due to ionic conduction and time-varying polarization, is

$$\vec{j} = (\sigma_s + i\omega\varepsilon_0\varepsilon(\omega))\,\vec{E} = \kappa(\omega)\vec{E},\ i = \sqrt{-1}, \qquad (1)$$

where ε_0 is the permittivity of vacuum. The additive contributions of ionic and polarization currents to the total current leads to a complex proportionality factor, denoted as κ in (1). It can be considered as a complex conductivity, $\kappa = \kappa' + i\kappa''$, where κ', κ'' are real and imaginary parts of this conductivity. They are given by

$$\kappa' = \sigma_s + \omega\varepsilon_0\varepsilon'' \text{ and } \kappa'' = \omega\varepsilon_0\varepsilon'. \qquad (2)$$

In (2) the standard decomposition $\varepsilon = \varepsilon' - i\varepsilon''$ has been used. Through the frequency dependence of the permittivity, real and imaginary parts of κ are frequency-dependent.

The schematic plots of κ' and $\varepsilon' = \kappa''/\omega\varepsilon_0$ vs. frequency in Fig. 1 show typical functional behavior of the real part of the conductivity and of the permittivity, the latter corresponding to the imaginary conductivity, for biological tissue.

There are three major relaxation regions, called α, β and γ, at frequencies of approximately 100 Hz, 500 kHz and 25 GHz. These regions are related to extracellular surface polarizations of large cells (α-region), to increasing capacitive charging and discharging of cell membranes (β-region) and to the relaxation of the water molecules (γ-region), respectively. At low frequencies the current is mostly extracellular, whereas with increasing frequencies intracellular contributions become increasingly significant, and the observations more cell-specific. The frequency dependence of the permittivity

[3] From AC circuits where phase shifts between current and voltage occur, complex notation is also known. Ohm's law is formulated as a relation between a complex voltage and a complex current with a complex proportionality factor, called impedance.

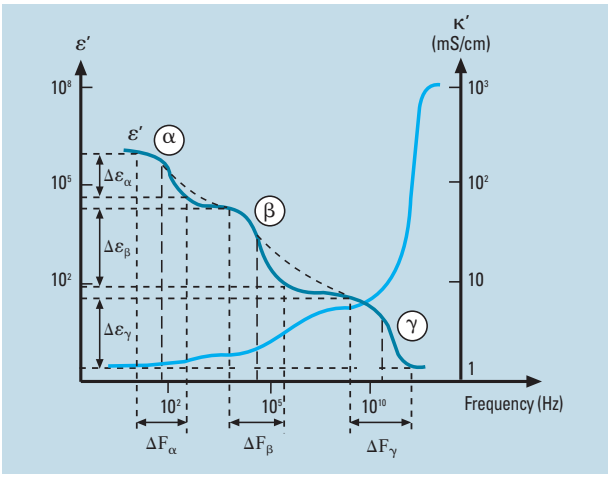

Figure 1
Ideal representation of permittivity and conductivity of biological tissue as a function of frequency. The three major relaxation regions, α, β and γ, are characterized by central frequencies F, and permittivity variations Δε. In practice, additional, smaller relaxation effects make the regions ΔF_α, ΔF_β and ΔF_γ overlap, and in extreme cases, the dotted curve from α to β to γ may be observed (Figure by permission of Begell House Inc.).

can be described by the so-called Cole-Cole parameters. Detailed explanations can be found in [7-9]. Since breast tissue conductivities measured *in vivo* are not available, we refer to the most recent *in vitro* measurements [4]. They were made at 12 frequencies, from 488 Hz to 1 MHz. The Cole-Cole parameters derived from these measurements are used to calculate the frequency dependence of the real parts of the conductivities and of the permittivities, and the imaginary parts of the conductivities for some tissues investigated in [4]. The graphs are plotted in Fig. 2-4.

The real part of carcinoma conductivity is only 3 to 6 times higher than that of adipose and connective tissue. This may be an unexpectedly low difference. The frequency behavior shows an increase in conductivity especially for carcinoma, as expected in the β-relaxation region. Since the lowest frequency at which the *in vitro* measurements were done was 488 Hz, the parameters from [4] cannot describe α-relaxation which is in the range of 100 Hz. Therefore, the curves in Fig. 2 do not show relaxation behavior at α-frequencies. The same argument holds for the permittivity curves, also derived from the parameters of Jossinet's article [4]. In Fig. 3 the decrease in permittivity is observed at β-relaxation frequencies. The curves in Fig. 2, 3 are to be compared with the ideal functional frequency behavior of Fig. 1. In the frequency range used in [4] a satisfactory agreement between ideal and measured curves is observed. In case of permittivities, the measured curves match more closely the dashed line of Fig. 1.

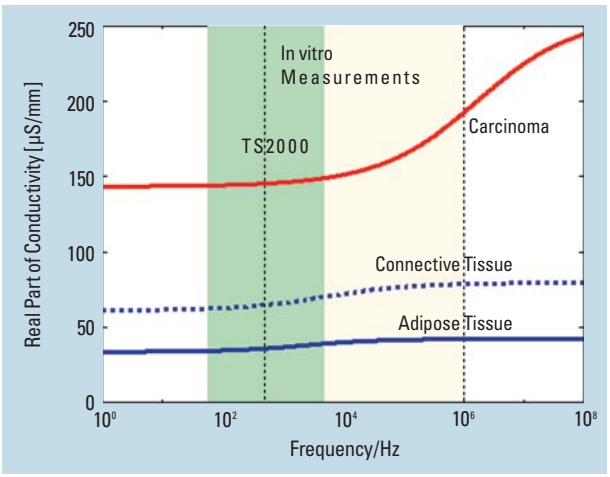

2

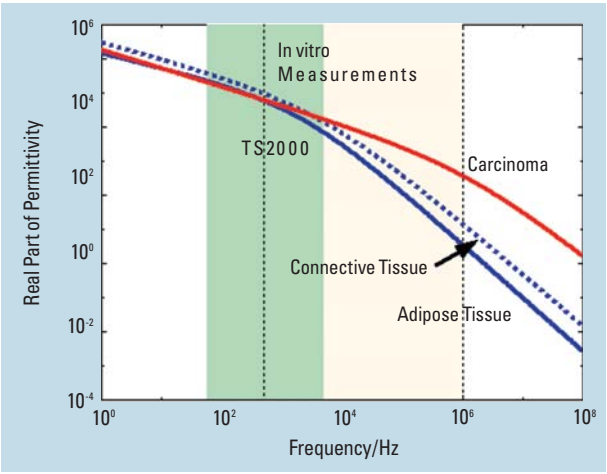

3

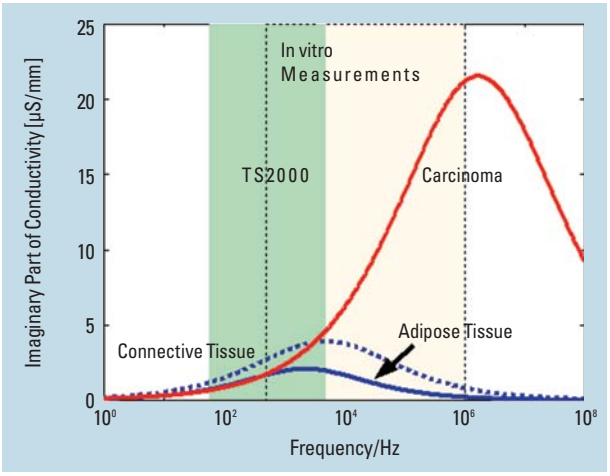

4

Figure 2
Real part of conductivity for various types of breast tissue calculated from parameters in [4].

The frequency range limited by dashed lines is the range of the *in vitro* measurements. The green area marks the frequency range currently accessible by the TransScan TS2000 system.

Figure 3
Real part of permittivity for various types of breast tissue calculated from parameters in [4]. Further remarks, see Fig. 2.

Figure 4
Imaginary part of conductivity for various types of breast tissue calculated from [4]. Further remarks, see Fig. 2.

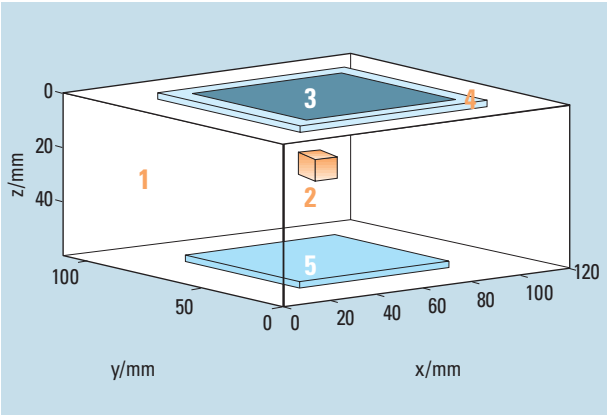

Figure 5
Simulation model for the breast with breast lesion and EIS measurement arrangement:

No.1 denotes the large cuboid representing the breast;
No. 2 denotes the lesion.

The measurement system has three components: the area of electrodes (3), the guard ring (4) – a metallic strip held at the same potential as (3) and surrounding (3) – and the reference electrode (5).

In the simulations presented in the next section complex conductivities are used. The imaginary parts of the conductivities of interest are shown in Fig. 4. The substantial difference between the electrical behaviors of malignant and healthy tissues is observed to increase with frequency.

There is a well known discussion of possible differences between *in vivo* and *in vitro* properties of biological tissue, i. e. on pages 75-76 of [7]. Clearly, differences are to be expected. However, since there are no *in vivo* measured conductivitites – not to be confused with conductances – available, the *in vitro* must suffice for further work, including as input for simulations.

Simulations

Simulation studies help to understand the essential conditions for the detectability of lesions by EIS measurements. Even a simple computational model is sufficient for explanation of the basic facts.

The results presented are obtained with a cuboid as breast model (Fig. 5). The lesions are represented as smaller cuboids in the breast cuboid. Their conductivities, tacitly assumed to be complex, are different from the surrounding areas. The squared measurement grid with equidistant electrodes (representing sensors on the probe) is on the top of the breast cuboid. The reference electrode (cylinder) is modeled as a planar plate placed on the bottom of the cuboid. Since the z axis depicts increasing depth, i. e. distance from the measurement grid, the z coordinate of the reference electrode is positive. In Fig. 5 the bottom of the cuboid is at $z = 56$ mm.

Throughout this section the conductivity of any lesion is that of cancerous tissue as discussed in the biophysics section. The surrounding conductive region is assumed to have adipose conductivity. The data are simulated at 200 Hz, the current standard frequency of the TransScan TS2000. Due to model limitations (e. g. geometry, *in vitro* conductivitites, unknown contact impedance between volume conductor and electrodes) measured and simulated data are not numerically identical. However, the results are expected to describe the functional dependencies on parameters such as size and depth of the lesion.

Current data simulation is done in multiple computational steps. First, the whole volume conductor is discretized in order to apply numerical methods. Secondly, the electrical potential in the whole volume conductor is calculated taking into account prescribed potential values on the measurement grid, e. g. 0 Volt, and at the reference electrode, e. g. 0.1-2.5 Volts. From the potential, the electric field and electric current density can be calculated at each grid point of the discretized cuboid. In accordance with the TransScan TS2000 data display, the simulated data, the magnitudes, and phases of the currents at the electrode sites are converted into conductance and capacitance values.

The conductance and capacitance data are displayed over a two-dimensional area representing the area of measurement. Thus, a map of data is shown. Alternatively, the data can be displayed as gray level "images". However, this terminology may be misleading, suggesting that EIS would be an imaging modality. The two-dimensional data measured at the surface of a region of interest cannot be considered as an image representing morphological structures. Therefore, we propose to denote these data as maps of impedance.

The simulations series starts with model configurations ensuring ideal lesion detectability. This case would be given if the electric field would be homogeneous in the absence of any lesion. It is realized if the top and the bottom area of the cuboid, the measurement area (3) and reference electrode (5) would have the same size, irrespective of the height of the cuboid, i. e. the thickness of the breast. If the breast is laterally larger than the probe area, the ideal detectability conditions would be distorted, the electric field would no longer be homogeneous.

Ideal detectability conditions enable the study of the isolated effects of parameter changes. Results of lesion detectability under such conditions are presented in Fig. 6 to Fig. 11. In Fig. 6 conductance maps of single lesions of the same size ($4 \times 4 \times 4$ mm^3) in increasing depths are shown[4]. As discussed qualitatively above, a

[4] It should be noted that depth is understood as the distance between the measurement grid and the center of gravity of the lesion. It is the z coordinate of the lesion's center of gravity.

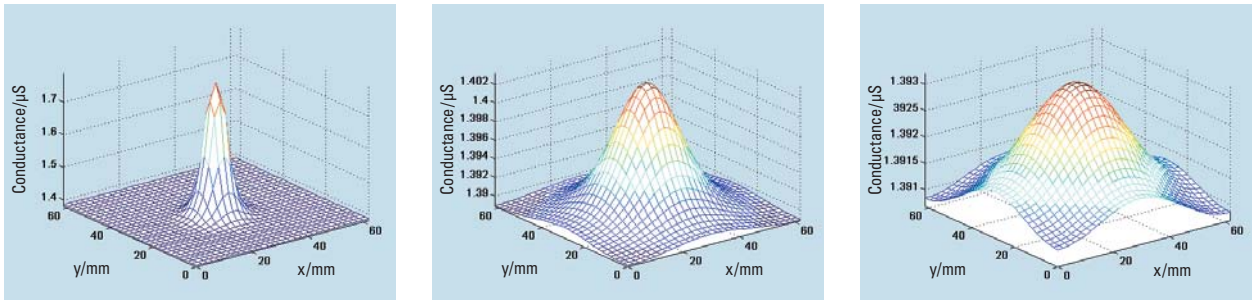

Figure 6
Fixed lesion size (4×4×4 mm³), increasing depth (distance between the center of gravity and the surface): impedance maps show decreasing signal heights. These maps are simulated under ideal detectability conditions.

lesion induces a signal enhancement measurable just above its location. When the data are displayed as a gray level image, the lesion is seen as a white spot (Fig. 7).

Throughout this article we present only conductance maps, since at the standard frequency of 200 Hz, no additional diagnostic information would be extracted from capacitance maps.

The expected decrease of the peak of the map and the increase of its broadness is shown in Fig. 6. There, different conductance scales have been chosen in order to visualize also the small signal enhancements of deep-lying lesions. In Fig. 8 the conductance rise (difference between peak and nearest local minimum value) are plotted against the depth of lesions of different sizes. For deep-lying lesions the signal rises can be better seen if the conductance scale is reduced (Fig. 9). For the simulated signal rises and for noise levels of about 0.03 µS, which should be obtainable after data averaging, small lesions (4×4×4 mm³) would theoretically be detected only up to a depth of about 2 cm. Larger lesions (8×8×8 mm³ and 12×12×12 mm³) would be detectable up to a depth of about 3 cm to 4 cm. In case of higher

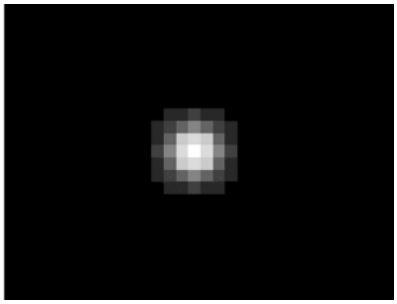

Figure 7
Gray level image of the first conductance map of Fig. 6.

The lesion shows up as a white spot.

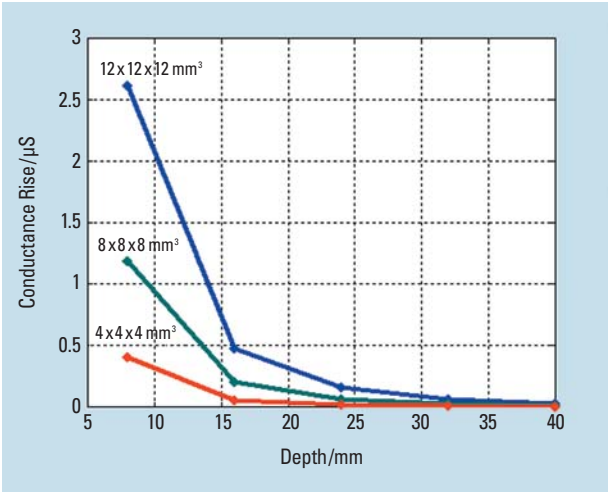

8

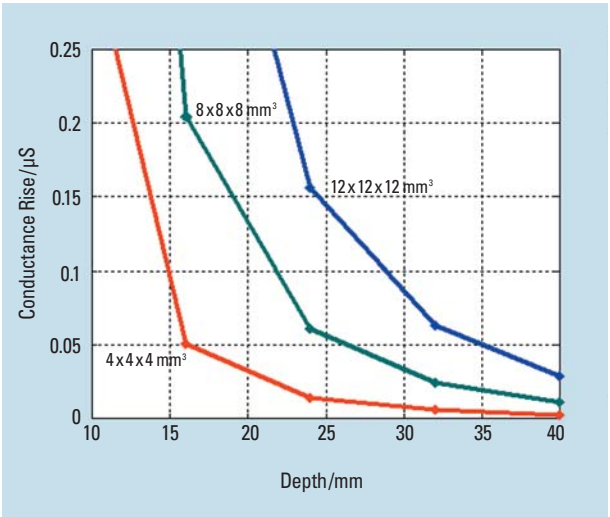

9

Figure 8
Conductance rise for lesions of different sizes in different depths. The 1st, 3rd and 5th data points of the 4×4×4 mm³ curve are from the maps of Fig. 6.

Figure 9
Plots of Fig. 8 for a different conductance scale. Lesion detectability decreases with increasing depth and increasing noise level.

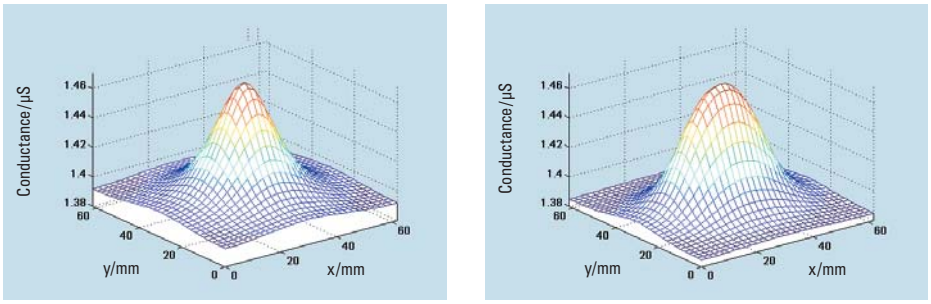

a b

Figure 10
Cuboid with dimensions of $4 \times 4 \times 24$ mm^3 generates orientation-dependent maps. In (a) the long side of the cuboid is parallel to the z axis, whereas in (b) it is the short side which is parallel to the z axis.

These distances between the upper boundary area of the cuboid and the measurement grid are the same in (a) and (b).

signal rises due to real higher conductivity of cancerous tissue, this lesion detectability would be possible without data averaging.

However, for non-spherical objects, the signal rise not only depends on their volumes considered so far, but also on their shapes and on their spatial orientations. This is immediately evident when cuboids of totally different dimensions are used in the simulation. For example, a cuboid with a base of 4×4 mm^2 and a height of 24 mm will yield orientation-dependent maps (see (a) and (b) of Fig. 10). In (a), the cuboid is oriented with its height dimension along the z axis; in (b), this side is parallel to the measurement plane. The distance between the upper boundary area of the lesion and the measurement grid is the same in both cases.

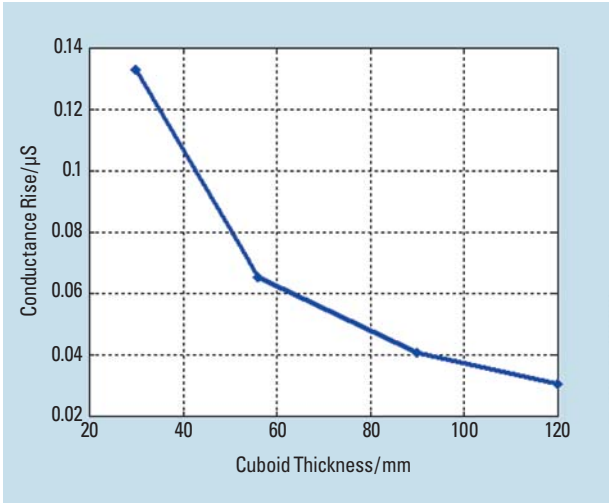

Figure 11
The effect of the z dimension of the volume conductor cuboid (breast thickness) on the peak value of impedance maps of a lesion.

The parameters of the lesion remained fixed. The maps were simulated under ideal detectability conditions.

As might be expected, the peak value of case (a) is slightly higher than that of case (b). Nevertheless, the signal rise is lower in (a) than in (b). This is due to the higher increase of the minimum value of (a) compared to that of (b), (Fig. 10). The reason is the small cross-sectional area exposed to the incoming currents in (a) as compared to (b). In situation (a) a large portion of current flows around the "attracting" inhomogeneity, such that the electrodes at the edges of the measurement array record higher signals than in (b), thus increasing the minimum value.

Another factor determining the signal maps is the thickness, i. e. the z extension, of the breast. For a lesion at fixed distance to the measurement grid and of fixed size, the peak value of its maps decreases with increasing breast thickness (Fig. 11). With increasing breast thickness, the current path through the breast tissue is longer, thus inducing a lower potential drop along the z extension of the lesion. Therefore, the lesion-induced change of the current is reduced.

If the top and bottom area of the cuboid are larger than the probe's area, the electric field would be inhomogeneous, even in the absence of a lesion in an otherwise homogeneous volume conductor. In this scenario (e. g. large breast), ideal detectability conditions of our simulations are not in effect. The lesion signals in the map become smaller with increasing surface (Fig. 12). This can be understood by the spread of the current in the entire volume, thus decreasing the current density in the region of the lesion. The plot of equipotential and field lines in Fig. 13 demonstrates this circumstance. In Fig. 13b a slight asymmetry of the potential lines can be observed. This is due to a 2 mm off-central positioning of the measurement grid.

This section will be concluded by considering noise. Noise includes electronic and biological noise. Assuming additive Gaussian noise with mean zero, and variance deduced from an 8-fold averaged TS2000 data, the map of Fig. 12b will change to the map of Fig. 14. As mentioned above, in case of higher signal rises due to enhanced cancerous lesion conductivity as compared to the Jossinet data, data averaging could be omitted, and still a detectable signal could be observed.

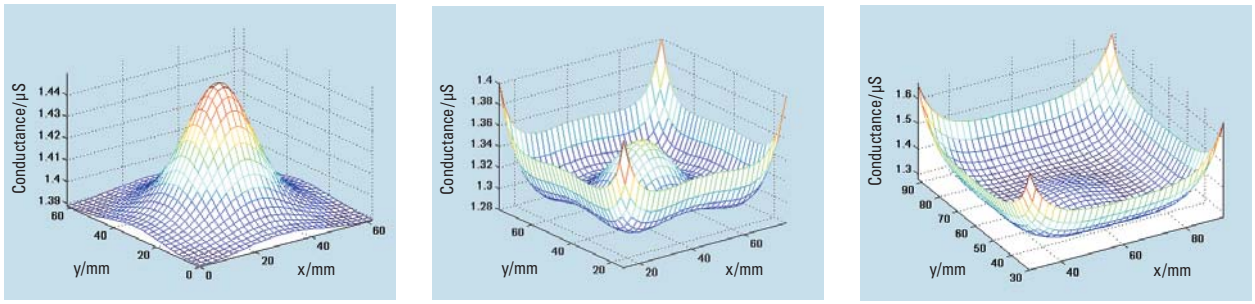

a b c

Figure 12
(a) to (c) depict the resulting signal maps when the top and bottom areas of the cuboid increase:
62×62 mm^2, 90×90 mm^2, 120×120 mm^2.

Due to the spread of the current in the entire cuboid and to the influence of edge effects, the lesion signals in the central part of the map decrease. The lesion is an $8 \times 8 \times 8$ mm^3 cuboid at a depth of 24 mm.

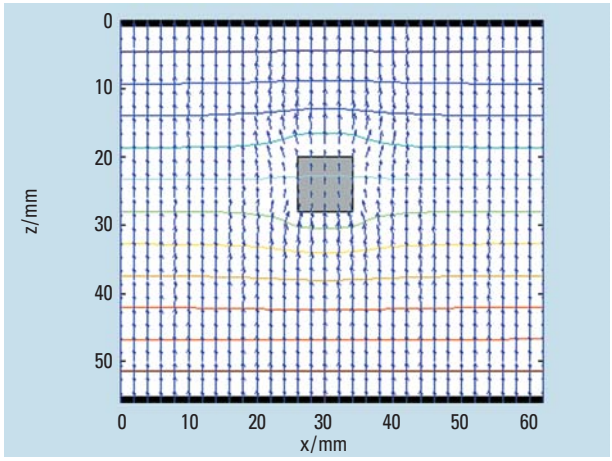

a

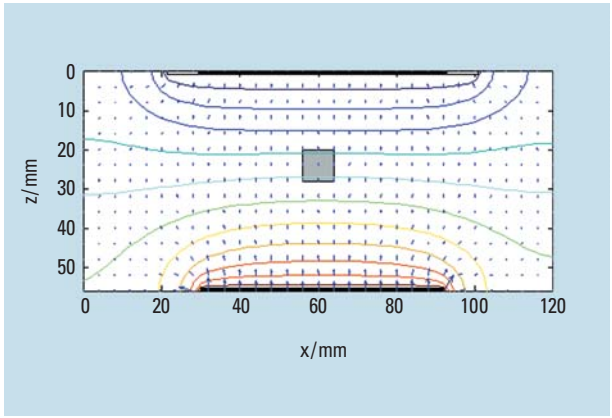

b

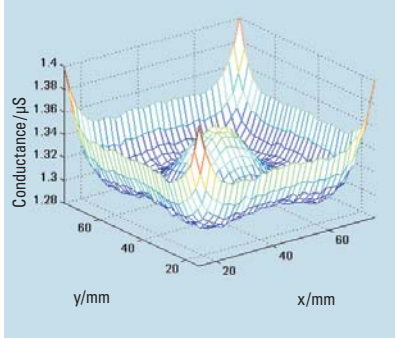

Figure 13
Equipotential and electrical field lines related to the maps (a) and (c) of Fig. 12.

Figure 14
Map of Fig. 12b after adding Gaussian noise of mean zero and variance taken from averaged TransScan TS2000 measurements.

The noise-corrupted map of Fig. 14 suggests that in EIS noise poses no serious problems. However, noise reduction due to data recording for averaging requires sampling time.

TS2000 – Electrical Impedance Scanner for the Breast

TransScan TS2000 (TransScan Medical, Ltd., Migdal Ha'Emek, Israel; distributed by Siemens AG) is the medical industry's first commercially available electrical impedance scanner (Fig. 15). The system comprises a main console (processor, additional processing module and power supply), a color monitor, data transfer devices, and two scanning probes. The unit is mobile on a trolley, and is approximately the size of a mid-range ultrasound unit.

The measurement tools are the scan probes and a reference electrode. The probes contain each a planar array of electrodes (16×16 and 8×8 on the large and small probes, respectively). Each electrode has an area of 3×3 mm^2. The center-to-center distance between electrodes is 4 mm, thus leaving a space of 1 mm between adjacent electrodes. The sensing area is surrounded by a metallic strip of 7 mm width, termed the guard ring, which hinders electrical edge effects. Thus, the total probe areas are 79×79 mm^2 and 47×47 mm^2 of large and small, respectively. The surface of the probe opposite to the sensing area includes a control panel with operator buttons for convenient use. The scan probe is connected to the console by means of a flexible cable.

The reference electrode is a metallic cylinder (diameter 3.4 cm, length 12 cm) which is held by the patient in her hand (Fig. 15).

Figure 15
Breast examination with the TransScan TS2000 breast scanner. The patient lies recumbent, holding the cylindric reference electrode in the hand contralateral to the examined breast.

Current flow through the breast is induced by a potential difference between probe electrodes and the reference electrode. The measuring electrodes are at ground potential. The potential of the reference electrode is adjusted automatically such that the current signals are optimal. However, safety regulations limit the voltage to 2.5 V and the current to 5 mA. The TS2000 currently operates with up to 30 voltage frequencies in the range from 58 Hz to 5 kHz. Signal quality requires use of a conductive gel as medium between sensing area and breast surface.

There are two resolution modes: standard and high resolution. In standard resolution mode (available only on the large probe), sub-arrays of 2×2 sensors are formed by summing the signals of these sensors. Thus, an 8×8 data array is obtained. In high resolution mode, the data of the 16×16 sensors (8×8 sensors in the case of the small probe) are processed independently and displayed in gray scale on the monitor.

Data quality is improved by repeated sampling, e. g. 2, 4 or 8 samples, over the array and by subsequent averaging. The data of each sensor, magnitude of the current and phase with respect to a reference signal, are converted to conductance and capacitance values assuming an RC circuit modeling the tissue.

The 8×8 or 16×16 impedance data, respectively, can be optionally interpolated and then be displayed in real-time as a gray level impedance map. Without interpolation, a blockwise 8×8 or 16×16 map is shown, whereas in the case of interpolation, a smoothed map is obtained.

During the examination the patient lies recumbent. She holds the reference electrode cylinder in her hand contralateral to the breast being examined. In the *scanning examination mode* the probe is guided in a pre-defined sequence by the operator to record 3×3 data sectors which cover the entire breast (Fig. 16). Scanning of both breasts, with the display of both conductance and capacitance of each, yields in total four 3×3 sector maps. The respective central sector maps the nipple region. Since conductivity of nipple tissue is very high (in accordance with intrinsic cell properties), the healthy nipple is always represented as a white spot.

The *targeted examination mode* is performed when the examination is limited to obtaining recordings at the region(s) of interest (Fig. 17). In this mode the recording positions are marked on an anatomical sketch and the related impedance maps are shown above this sketch.

The examination time is short; acquisition, processing of the data and display of the result are in real time.

As explained above, cancerous tumors cause enhanced current signals measured by the nearest sensing electrodes when the electrode array is placed above the lesion. A set of algorithms translates the quantitative data sets (measurements) to yield gray-scale images, where the cancer signal is visualized as a focal white spot.

Not to be ignored is the fact that other factors, including skin-surface lesions (e. g. mole, pimple, scar), bone (costochondral junction, inframammary ridge, ribs), and hormone-related tissue changes, can cause enhanced current signals, and therefore appear as artifacts. The images must be interpreted by a qualified and trained clinician, who takes into account the results of all available examinations when determining the diagnosis.

Discussion

The aim of this article was to review the physical basis of EIS. It was presented how, in principle, lesions with conductivities different from the surrounding tissue cause electric field distortions in their surrounding tissues. Depending on the size, depth and conductivity ratio with respect to the surrounding, these distortions lead to current signals measurable on the skin surface at the region of interest.

Since malignant lesions do indeed have electric properties different from healthy tissue, these lesions can generate detectable signals. This qualitative reasoning of the measurement priciples section has been confirmed by a variety of numerical simulations.

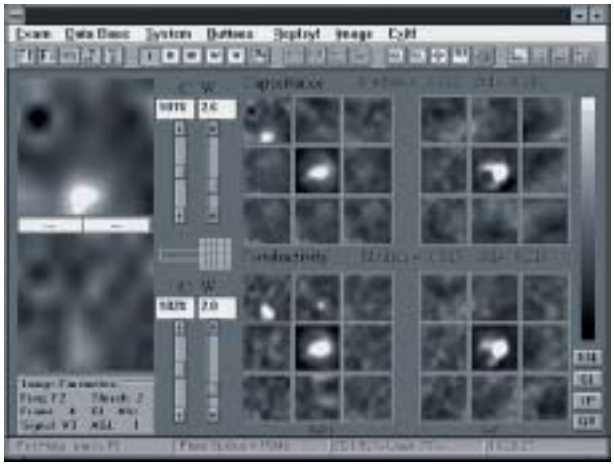

Figure 16
Screen display in the scanning mode. Sector maps of the right and left breast are shown on the left and right side corresponding to the operator's view of the patient. Individual sectors can be selected and examined in greater detail.

Figure 17
Screen display in the targeted mode. The region of interest (lesion, suspected lesion) is scanned, and independently recorded. Up to five sectors are saved, their locations corresponding to numbered positions on the anatomic sketch.

The simulation model is simplified. However, it exhibits essential features such as bounded volume, inflow of current from the bottom, i. e. from the thoracic muscle region, and inhomogeneous conductivity regions. Nevertheless, numerical differences between simulated and real data should not be surprising due to geometrical and electrical model errors. The geometry and the conductivity distribution of the breast model might be too simple.

The simulations require conductivities as input parameters. As mentioned, the most recent *in vitro* data [4] have been considered. We are aware of additional discrepancies between simulated and real data due to the *in vitro* conductivity values assumed. To the best of our knowledge, no *in vivo* conductivity data have been reported in the literature. In [5] and [6] *in vivo* resistance and capacitance measurements are published. The derivation of impedivity (the inverse of complex conductivity) data requires geometry factors not yet obtainable from *in vivo* measurements.

The signals measured with the square array of electrodes are displayed in an image-like manner. They are, however, by no means images of biophysical quantities, i. e. of the conductivity. The ensemble of signals should be interpreted as a surface *map* of electric signals reflecting inhomogeneities in conductivity beneath the measurement array. They generate peaks or hollows in the maps depending on their sizes, depths and conductivities with respect to their surroundings. It is meaningless to discuss image quality of the gray level representations of the derived impedance distributions.

The clinical relevance of the EIS method has been evaluated with the TransScan TS2000 system, and its predecessor, known as Mammoscan. The TS2000 was granted FDA approval for adjunctive use with X-ray Mammography [10], achieving in combination reported sensitivity and specificity of 90% and 77%, respectively [10].

Nissan, et al. presented improvement of 8 % in sensitivity when EIS was used in combination with Mammography [11]. In a study of 583 biopsy cases, Moskovitz reported TransScan specificity ranging from 64-71% for the various subpopulations; comparable mammographic specificity in this group was 26-40% [12]. Other studies report similar statistics [13, 14].

Further clinical applications, such as the use of this technique for evaluation of lymph nodes, are of interest. Malich, et al. conducted a study on the use of EIS for the classification of malignant/benign lymph nodes, and reported an achieved sensitivity of 93%, with a specificity of 62.8% [15].

Although the clinical results are encouraging, there are problems to be solved and further improvements to be implemented, the most critical of which is the reduction of false positive findings, or artifacts. This may

be addressed with the use of frequency dependencies of data for diagnosis. To date, the multifrequency behavior of impedance has not been systematically used. There are ongoing activities, both at TransScan Medical and Siemens AG, to develop specialized algorithms to evaluate the complete information content of the data. Based on published data and clinical experience, expectations are justified that the diagnostic capabilities of the EIS method will be considerably enhanced through this research.

Literature

[1] Singh, B., Smith, C. W., Hughes, R.: *In vivo* dielectric spectrometer. Med. & Biol. Eng. & Computing 1979; 17:045-060.

[2] Surowiec, A. J., Stuchly, S. S., Barr, J. R., Swarup, A.: Dielectric Properties of Breast Carcinoma and the Surrounding Tissues. IEEE Trans. Biomed. Eng. 1988; Vol 35, No. 4:257-263.

[3] Jossinet, J.: Variability of impedivity in normal and pathological breast tissue. Med. & Biol. Eng. & Computing 1996; 34:346-350.

[4] Jossinet, J.: The impedivity of freshly excised human breast tissue. Physiol. Meas. 1998; 19:61-75.

[5] Morimoto, T., Kinouchi, Y., Iritani, T., Kimura, S., Konishi, Y., Mitsuyama, N., Komaki, K., Monden, Y.: Measurement of the Electrical Bio-Impedance of Breast Tumors. Eur. Surg. Res.1990; 22:86-92.

[6] Morimoto, T., Kimura, S., Konishi, Y., Komaki, K., Uyama, T., Monden, Y., Kinouchi, Y., Iritani, T.: A Study of the Electrical Bio-impedance of Tumors. J. Investig. Surg. 1993; 6:25-32.

[7] Foster, K. R., Schwan, H. P.: Dielectric Properties of Tissues and Biological Materials: A Critical Review. Critical Reviews in Biomedical Engineering 1989; Vol. 17, Issue I:25-104.

[8] Stuchly, M. A., Stuchly, S. S.: Electrical Properties of Biological Substances. Biological Effects and Medical Applications of Electromagnetic Energy. Ed. Om P. Gandhi, Prentice Hall Inc., Eaglewood Cliffs, NJ, USA, 1990.

[9] Morucci, J. P., Valentinuzzi, M. E., Rigaud, B., Felice, C. J., Chauveau, N., Marsili, P. M.: Bioelectrical Impedance Techniques in Medicine. Critical Reviews in Biomedical Engineering, Vol. 24, Issues 4-6:275, Begell House Inc., Congers, NY, USA, 1996.

[10] Transcan T-Scan 2000 Gets Panel Nod As Mammography Adjunct, The Gray Sheet 1998; Vol 24, No. 34:5-6.

[11] Nissan, A., Spira, R. M., Freund, H. R., Fields, S. I.: Imaging of the Breast with Electrical Impedance Scanning as an Adjunct to Mammography. Scientific Presentation, Senology Congress, Cancun, Mexico, May 2000.

[12] Moskovitz, O.: T-Scan 2000 Breast Impedance Imager, New Adjunct to Mammography for Breast Cancer Detection. Review of 583 Biopsy Cases, unpublished manuscript, Feb. 1998.

[13] Malich, A., Facius, M., Marx, C., Böhm, T., Freesmeyer, M., Fleck, M., Kaiser, W. A.: Electrical Impedance Scanning – Clinical Value in the Verification of Uncertain Breast Lesions. European Radiology. 2000; Vol. 10, No. 9:F51..

[14] Malich, A., Boehm, T., Facius, M., Freesmeyer, M., Fleck, M., Anderson, R., Kaiser, W. A.: Differentiation of mammographically suspicious lesions: Evaluation of Breast Ultrasound, MR Mammography and Electrical Impedance Scanning as adjunctive technologies in breast cancer detection. Submitted to Clinical Radiology, 2000.

[15] Malich, A., Facius, M., Fritsch, T., Freesmeyer, M., Marx, C., Rott, A., Fleck, M., Anderson, R., Kaiser, W. A.: Die elektrische Impedanzmessung – ein neues additives Verfahren zur verbesserten Differenzierung unklarer Lymphknotenschwellung. Vortrag, Deutscher Röntgenkongreß, Mai 2000.

Siemens is a full-service distributor of TransScan medical products. The TransScan product is not distributed by Siemens Medical Systems in the United States.

Author's address

Dr. Bernhard Scholz
Siemens AG, Medical Engineering Group
Basic Research & Development Department
Henkestraße 127, D-91052 Erlangen, Germany
Phone: +49-9131 84 6637
Fax: +49-9131 84 4771
Email: Bernhard.Scholz@med.siemens.de